SUPPLEMENTARY MATERIALS
(Supplementary Movies, Figures, Appendix B, Supplementary References)

Optical mapping of optogenetically shaped cardiac action potentials

Sarah A. Park[1], Shin-Rong Lee[2], Leslie Tung[3], David T. Yue[1,2,3,4*]

[1] Program in Cellular and Molecular Medicine, The Johns Hopkins University School of Medicine, Baltimore, MD, USA.
[2] Department of Biomedical Engineering, The Johns Hopkins University School of Medicine, Baltimore, MD, USA.
[3] Department of Neuroscience, The Johns Hopkins University School of Medicine, Baltimore, MD, USA.
[4]Center for Cell Dynamics, The Johns Hopkins University School of Medicine, Baltimore, MD, USA.

[*] Correspondence and requests for materials should be addressed to D.T.Y. (dyue@jhmi.edu)

Supplementary Movie S1. ChR2-blue_pulses_excite_NRVM_monolayer.MOV
ChR2 lentivirus infected NRVM monolayer is excited with multiple short-duration, high-intensity blue light pulses. Excitation is observable as contractions. Background image appears red because the bright field light was filtered with a 760 nm long-pass filter to reduce ChR2 activation by background blue wavelengths.

Supplementary Movie S2. eNpHR3p0-green_pulses_silence_and_elicit_anode-break-like_stimulation.MOV
eNpHR3.0 lentivirus infected NRVM monolayer is electrically stimulated at regular intervals (audible beeps), as observed by the contractions. A long-duration, high intensity green light pulse silences two expected contractions. The cessation of the green light pulse elicits an anode-break-like contraction. Successive short-duration, high intensity green light pulses also elicit anode-break-like contractions that are unsynchronized from the electrical pacing. Near the end, a short green light pulse causes an anode-break-like contraction that must have left the tissue refractory, such that an electrical stimulus cannot cause the tissue to contract. Background image appears red because the bright field light was filtered with a 760 nm long-pass filter to reduce eNpHR3.0 activation by background green or yellow wavelengths.

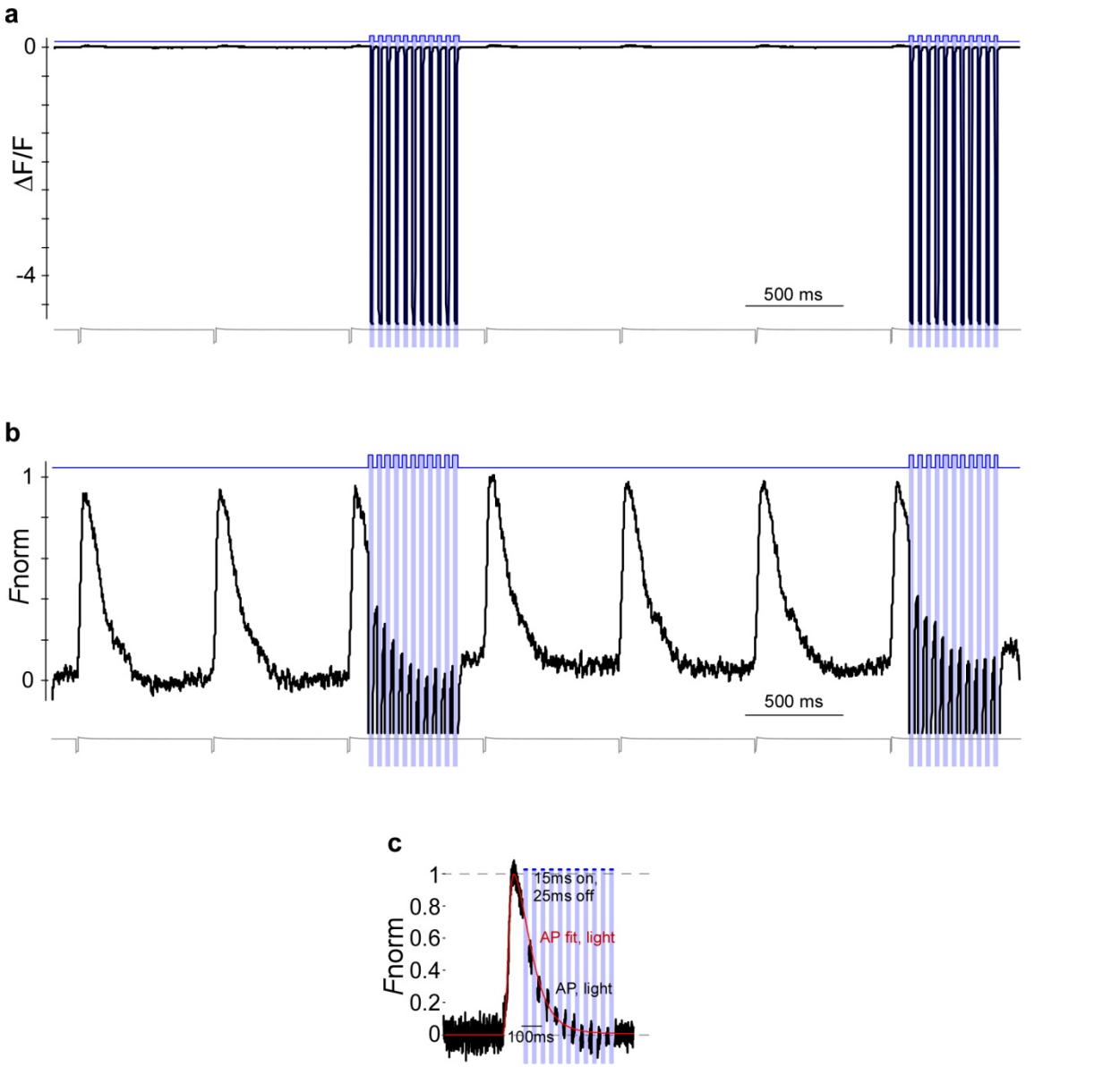

Supplementary Figure S1. The need for crosstalk compensation of blue light pulses (15 ms on, 25 ms off) during action potentials. (**a**) Exemplar optical mapping trace from one electrically paced channel showing the fluorescence baseline shift that occurs in the action potential signal when blue light pulses (blue trace) are turned on. Uninfected NRVMs. Traces were baseline subtracted and detrended with no normalization or filtering. Electrical pacing in gray. (**b**) Close-up of the same trace in A to better visualize the effect of the fluorescence baseline shift in the action potential signal when blue light (blue trace) is on. Traces were baseline subtracted, detrended, and normalized to a range from 0 to 1 based on the red light baseline and maximum signal amplitude, and filtered with a 15-point moving average filter. Electrical pacing in gray. (**c**) The 3rd action potential was selected from the signal shown in **b**, to illustrate the process of crosstalk compensation (black). The baseline shifts were removed from the signal (black) and the action potential was curve fitted to a 3-part Hill function (red). All blue illumination at 7.2 mW/mm^2.

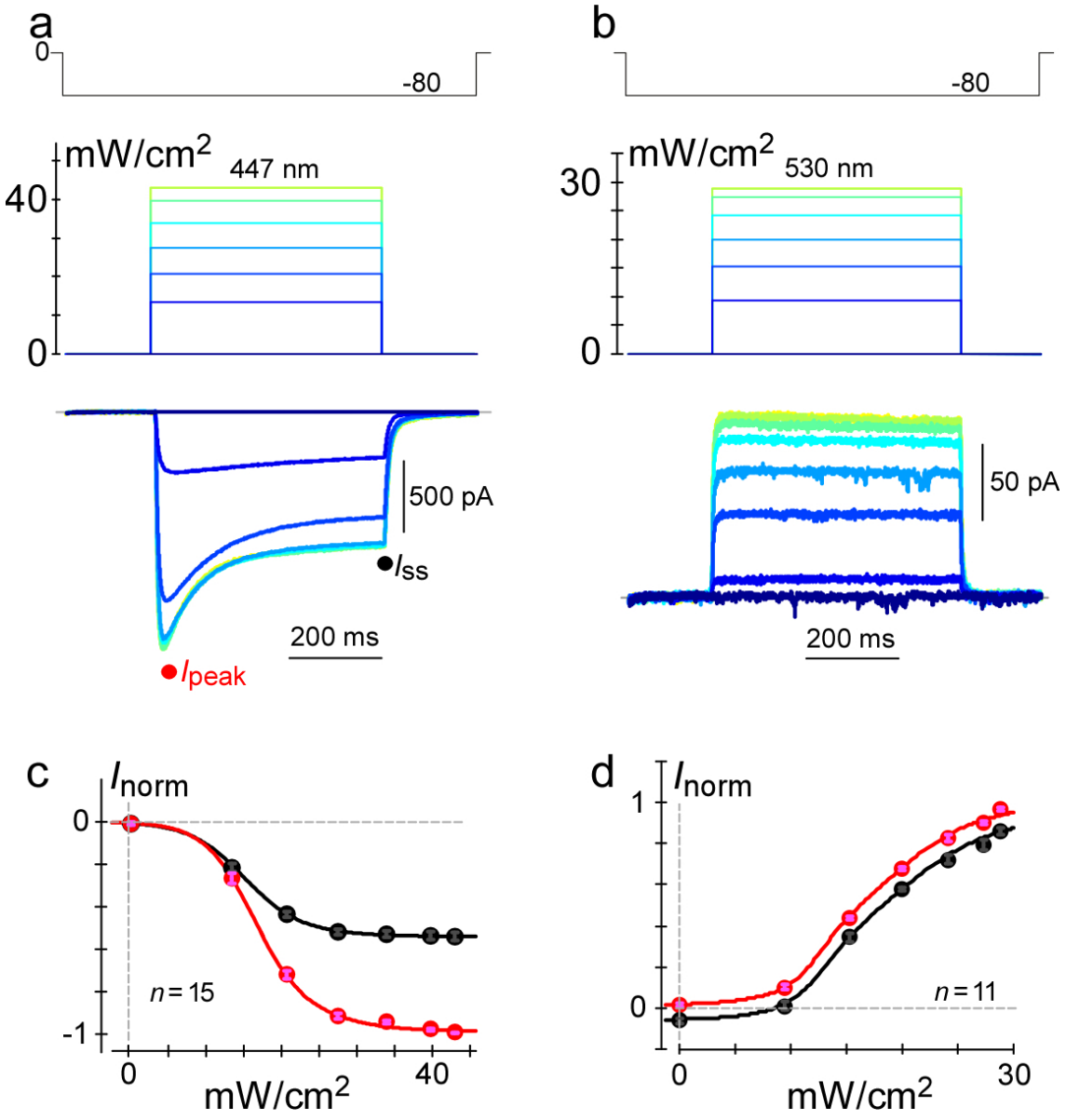

Supplementary Figure S2. Light intensity-dependence of optogenetic constructs. ChR2 (**a, c**) and eNpHR3.0 (**b, d**) were characterized at various constant levels of intensity during a voltage step of -80 mV, using whole-cell patch clamp in HEK293 cells. (**a**) ChR2 supports light-gated, light intensity- and voltage-dependent currents. Partial inactivation of currents is clearly present. (**b**) eNpHR3.0 is also light-gated and light intensity-dependent. (**c**) ChR2 population data for peak (red) and steady-state (black) current levels, normalized to peak current at maximum light intensity. (**d**) eNpHR3.0 population data for peak (red) and steady-state (black) currents, normalized to peak current at maximum light intensity.

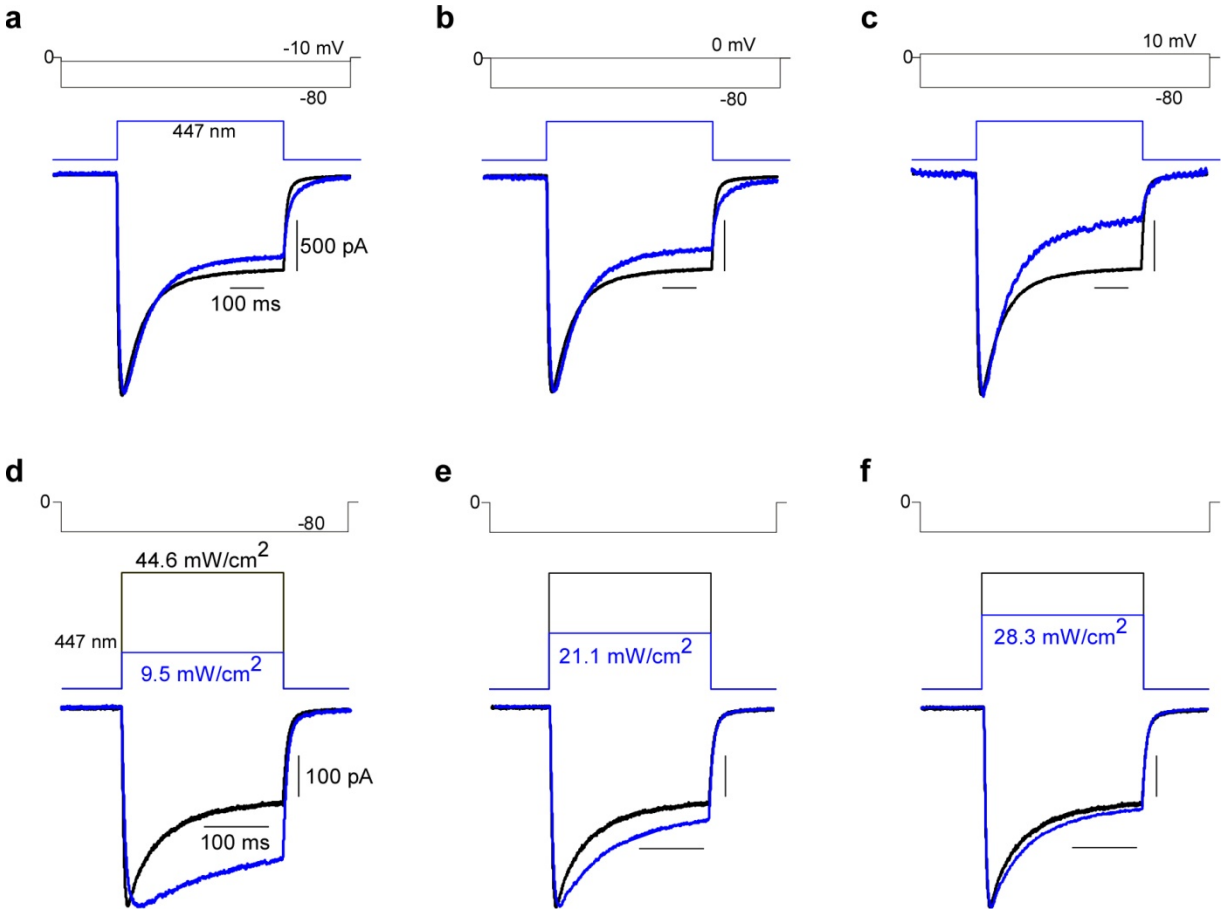

Supplementary Figure S3. Inactivation kinetics of ChR2 varies according to voltage and light intensity. (**a-c**) Comparison of inactivation kinetics of ChR2 according to voltage. Currents were acquired at various constant levels of voltage with blue light on at maximum intensity (44.6 mW/cm^2), using whole-cell patch clamp in HEK cells. Current traces in gray have been normalized to the peak of the black trace for comparison. Scale bars represent time and current for the black trace. (**a**) ChR2 current traces at -80 mV (black) and -10 mV (gray). (**b**) ChR2 current traces at -80 mV (black) and 0 mV (gray). (**c**) ChR2 current traces at -80 mV (black) and 10 mV (gray). (**a-c**) ChR2 inactivation is greater with increasing voltage. (**d-f**) Comparison of inactivation kinetics of ChR2 according to light intensity. Currents were acquired at a constant level of -80 mV with variable blue light intensities, using whole-cell patch clamp in HEK cells. Current traces in gray have been normalized to the peak of the black trace for comparison. Scale bars represent time and current for the black trace. (**d**) ChR2 current traces acquired with blue light intensity of 44.5 mW/cm^2 (black) and 9.5 mW/cm^2 (gray). (**e**) ChR2 current traces acquired with blue light intensity of 44.5 mW/cm^2 (black) and 21.1 mW/cm^2 (gray). (**f**) ChR2 current traces acquired with blue light intensity of 44.5 mW/cm^2 (black) and 28.3 mW/cm^2 (gray). (**d-f**) ChR2 inactivation is greater with higher intensity blue light.

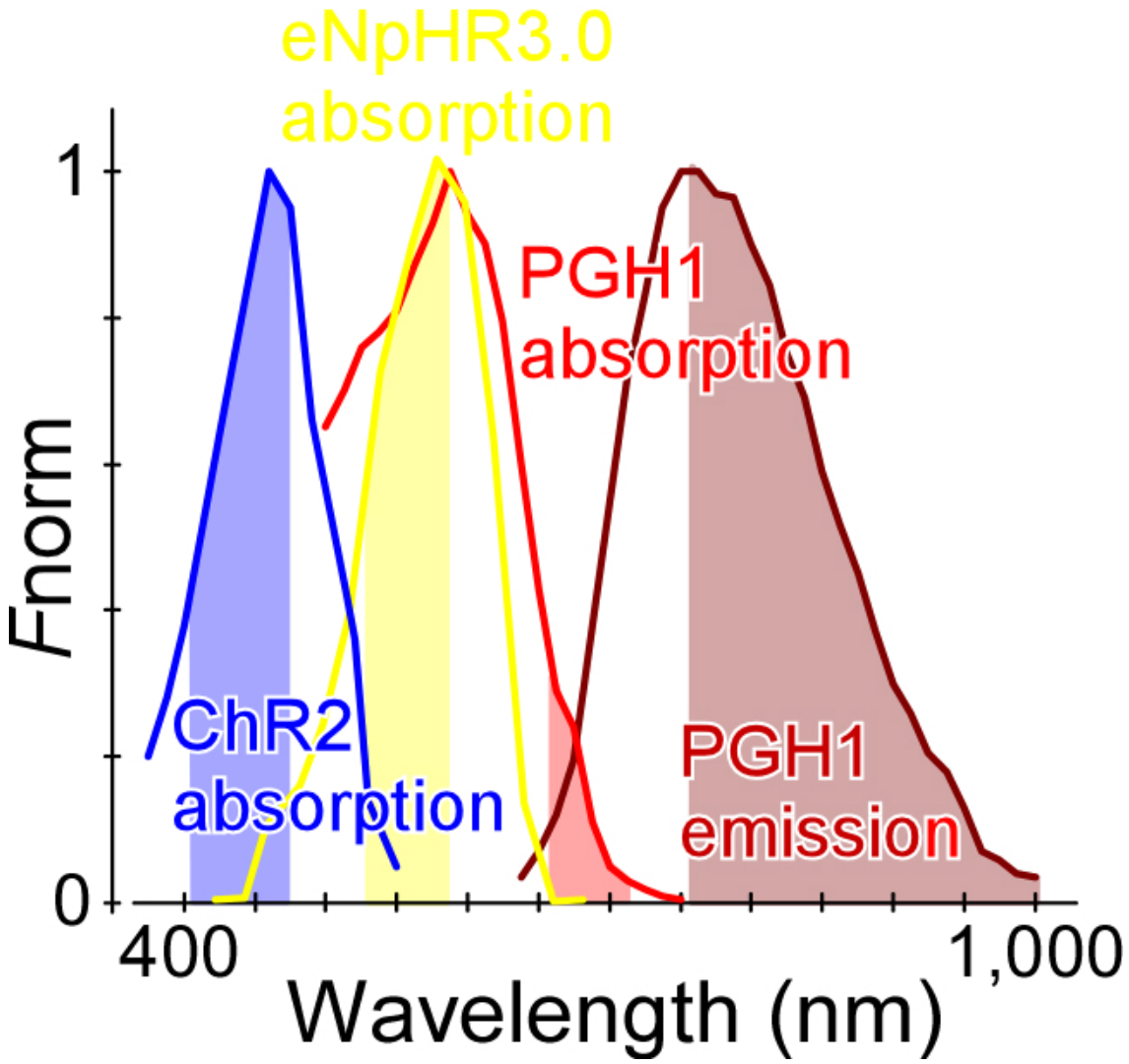

Supplementary Figure S4. Absorption and emission spectra of the optogenetic constructs and the long-wavelength voltage-sensitive dye re-created from [1-3]. The absorption spectrum of ChR2 (blue) is blue-shifted so that there is minimal crosstalk with the absorption spectrum of eNpHR3.0 (yellow). Absorption spectrum (red) and emission spectrum (dark red) of voltage-sensitive dye, PGH1. Optical filters helped to prevent crosstalk between the optogenetic constructs and PGH1. ChR2 was activated using a blue LED bandpass filtered between 410-470 nm (shaded blue area). eNpHR3.0 was activated using a green LED bandpass filtered between 535-585 nm (shaded yellow area). PGH1 was activated using a red LED bandpass filtered between 660-720 nm (shaded red area). Emission was collected with a longpass filter at 760 nm (shaded dark red area).

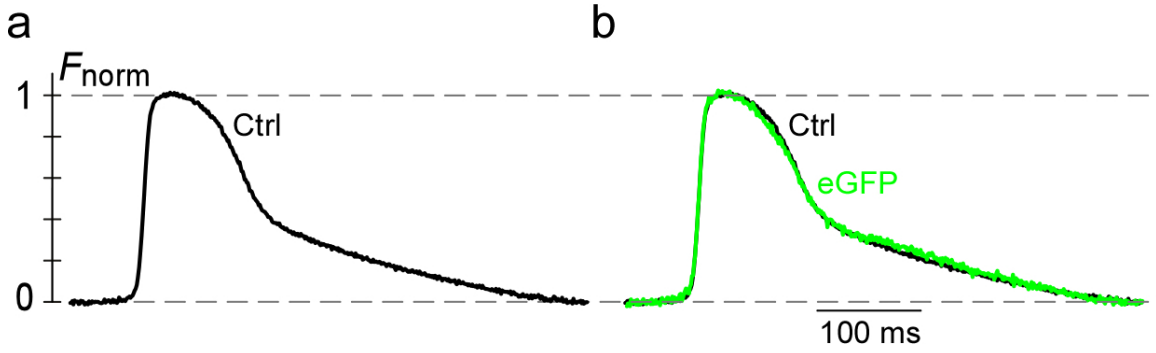

Supplementary Figure S5. Transduction of NRVM monolayers with empty lentivirus bearing only eGFP did not appreciably perturb action potential morphology from control (absent optogenetic stimulation with blue or green light). (**a**) Control NRVMs without viral transduction. Action potentials were averaged from multiple channels of optical mapping data, with di-4-ANEPPS as dye. (**b**) Results for NRVM transduced with empty lentivirus bearing only eGFP; format as in **a**. Parallel culture to un-transduced monolayer. Action potential (green) essentially unchanged from control (black), as reproduced from panel **a**.

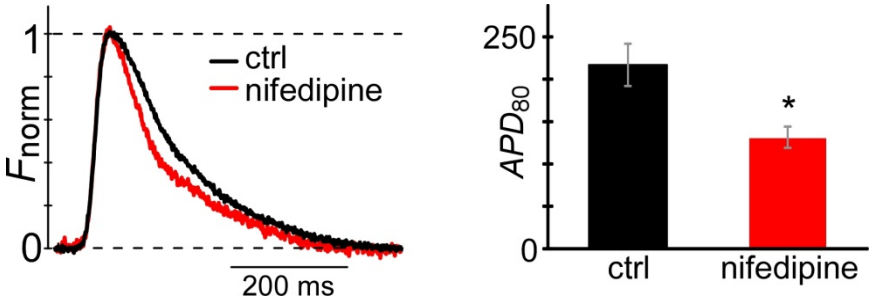

Supplementary Figure S6. Effect of L-type channel inhibitor nifedipine (1 μM) to shorten action potential that was optically recorded from control NRVM monolayer expressing only eGFP. The left subpanel displays the responses for an exemplar coverslip. The right subpanel displays the summary of duration analysis averaged over $n = 2$ coverslips. *, $p < 0.01$.

Appendix B

Relation of ion-channel conductances and sensitivity of $V_{plateau}$ changes to optocurrents

Here, we address the question of whether the disturbance of voltage at the plateau phase of an action potential by the injection of optogenetic currents, is a property of total ion channel conductance and/or the net ionic current.

We start with an equation by representing the time derivative of voltage at or near the action-potential plateau. This expression equals to the sum of ionic currents and the optogenetic current. Since there is litle time-dependent change in voltage at the plateau, we set the equation to zero as an approximation. G_i is a constant representing the conductance for each type of ion channel. V_p represents the plateau voltage. V_i represents the reversal potential of each type of ion channel. I_{opto} represents the optogenetic current during light excitation. C_m represents the membrane capacitance.

$$\frac{dV}{dt} = \frac{-\sum_i G_i (V_p - V_i) - I_{opto}}{C_m} = 0$$

The terms in the equation are rearranged to isolate for V_p, where G_T represents total conductance.

$$V_p = \frac{-I_{opto} + \sum_i V_i G_i}{G_T}$$

Finally, we differentiate in terms of I_{opto}.

$$\frac{dV_p}{dI_{opto}} = -\frac{1}{G_T}$$

Here, we see that the plateau phase voltage changes linearly as a function of injected optogenetic current, with scaling factor equal to the reciprocal of total ion-channel conductance. G_T is relatively small during the resting phase and plateau phase of human-like action potentials[4]. In NRVMs, the same would hold true, but G_T is likely somewhat larger at the peak of the action ptoential, compared to at the resting potential, due to substantial activation of voltage-gated K channels in NRVMs[5].

Supplementary References

1 Boyden, E. S., Zhang, F., Bamberg, E., Nagel, G. & Deisseroth, K. Millisecond-timescale, genetically targeted optical control of neural activity. *Nat Neurosci* **8**, 1263-1268 (2005).

2 Patrick, M. J. *et al.* Enhanced aqueous solubility of long wavelength voltage-sensitive dyes by covalent attachment of polyethylene glycol. *Org Biomol Chem* **5**, 3347-3353 (2007).

3 Zhang, F., Wang, L. P., Boyden, E. S. & Deisseroth, K. Channelrhodopsin-2 and optical control of excitable cells. *Nat Methods* **3**, 785-792 (2006).

4 Weidmann, S. Effect of current flow on the membrane potential of cardiac muscle. *J Physiol* **115**, 227-236 (1951).

5 Knollmann, B. C., Schober, T., Petersen, A. O., Sirenko, S. G. & Franz, M. R. Action potential characterization in intact mouse heart: steady-state cycle length dependence and electrical restitution. *Am J Physiol Heart Circ Physiol* **292**, H614-621, doi:10.1152/ajpheart.01085.2005 (2007).